Investigating the role of receptor interacting protein kinase 3 in venous thrombosis

Elise DeRoo, MD,[a] Mitri Khoury, MD,[a,*] Ting Zhou, PhD,[a] Huan Yang, PhD,[a] Amelia Stranz, BS, MS,[a] Catherine Luke, LVT, LAT,[b] Peter Henke, MD,[b] *and* Bo Liu, PhD,[a] *Madison and Ann Arbor, MI*

ABSTRACT

Objective: Venous thromboembolism is a disease that encompasses both deep vein thrombosis and pulmonary embolism. Recent investigations have shown that receptor interacting protein kinase 3 (RIPK3), a protein known for its role in the programmed form of cell death necroptosis, may play a role in thrombosis. Specifically, RIPK3 has been shown to promote platelet activation in arterial thrombosis and mixed lineage kinase domain-like pseudokinase (MLKL), a protein downstream of RIPK3 in the necroptosis pathway, has been shown to promote neutrophil extracellular trap formation in deep vein thrombosis. This investigation sought to comprehensively investigate the role of RIPK3 in deep vein thrombogenesis.

Methods: The inferior vena cava ligation and stenosis models of deep vein thrombosis were used in C57BL/6J, RIPK3 wild-type (*Ripk3*$^{+/+}$) and RIPK3-deficient (*Ripk3*$^{-/-}$) mice. Downstream tissue analyses included measurement of thrombus weight and histological and Western blot analysis of tissues for markers of necroptosis and cell death. A subset of C57BL/6J mice were treated with a RIPK3 inhibitor to determine the effect on venous thrombosis.

Results: C57BL/6J mice showed significant increases in thrombus weight from 6 to 48 hours. During the same time frame, RIPK3 progressively accumulated in the vein wall (a 35-fold increase from 0 to 48 hours). RIPK3 was present in the thrombus; however, it decreased with time. Although present in the thrombus, MLKL was nearly undetectable in the vein wall by Western blot at any timepoint. Immunostaining confirmed the high accumulation of RIPK3 in the vein wall, primarily colocalized to endothelial and smooth muscle cells. Phosphorylated MLKL, the active form of MLKL and executioner of necroptotic cell death, was detectable by immunostaining in the thrombus, but was present at low to undetectable levels in the vein wall. Propidium iodide and terminal deoxynucleotidyl transferase dUTP nick end labeling staining revealed a high burden of necrotic and apoptotic cells within the thrombus at 48 hours, but a relatively lower burden within the vein wall. Despite robust accumulation of RIPK3 within the vessel wall and the thrombus, knockout and inhibition of RIPK3 failed to impact thrombus incident or weight at 48 hours after inferior vena cava ligation. Neutrophil extracellular trap burden did not differ between *Ripk3*$^{+/+}$ and *Ripk3*$^{-/-}$ mice.

Conclusions: In mice, the vein wall responded to deep vein thrombosis induction with elevation of RIPK3 without showing markers of necroptosis and apoptosis. Studies using genetic or pharmacological inhibition of RIPK3 suggest that this cell death mediator may not have a major role in the acute phase of venous thrombogenesis. Further investigation is needed to determine if RIPK3 plays a potentially non-necroptotic role within the vein wall during later stages of thrombus resolution and vein wall remodeling. (JVS—Vascular Science 2022;3:365-78.)

Clinical relevance: Venous thromboembolism, encompassing deep vein thrombosis and pulmonary embolism is a major clinical problem, affecting approximately 1 million patients in the United States annually. Understanding the cellular and molecular mechanisms that drive deep vein thrombosis is critical to being able to develop future targeted therapies that not only prevent thrombus propagation, but also accelerate thrombus resolution and prevent adverse post-thrombotic vein wall remodeling without undue bleeding risks. Necroptosis, a form of programmed cell death, has been suggested to play a pathologic role in venous thrombus formation. This study investigates the role of the necroptotic protein receptor interacting protein kinase 3 in venous thrombosis.

Keywords: Venous thrombosis; Mouse model; Vein wall; Necroptosis; Cell death

From the Department of Surgery, and Department of Cellular and Regenerative Biology, School of Medicine and Public Health, University of Wisconsin-Madison, Madison[a]; and the Department of Surgery, Division of Vascular Surgery, University of Michigan, Ann Arbor.[b]

*Current address: Division of Vascular Surgery, Massachusetts General Hospital, Boston, MA.

Supported by the National Institutes of Health (R01HL149404 and R01HL158073 to B.L., and F32HL158171 to E.D.) and the American Heart Association (20TPA35490307 to B.L., and 20CDA35350009 to T.Z.).

Presented at the 2021 Vascular Research Initiatives Conference, San Diego, California, August 18-21, 2021.

Correspondence: Bo Liu, PhD, University of Wisconsin-Madison, 1111 Highland Ave, WIMR 5137, Madison, WI 53705 (e-mail: liub@surgery.wisc.edu).

The editors and reviewers of this article have no relevant financial relationships to disclose per the JVS-Vascular Science policy that requires reviewers to decline review of any manuscript for which they may have a conflict of interest.

2666-3503

https://doi.org/10.1016/j.jvssci.2022.09.002

Venous thromboembolism (VTE), which includes deep vein thrombosis (DVT) and pulmonary embolism is a common vascular disease that impacts up to 900,000 individuals in the United States annually.[1,2] The incidence of DVT varies substantially by race, sex, and age, ranging from an annual incidence of less than 1.49 per 1000 in those aged less than 45 years, to 5.00 to 6.00 per 1000 in those aged more than 80 years.[1] VTE is associated with substantial morbidity and mortality. An estimated 25% of patients with pulmonary embolism present with sudden death, and 30% to 50% of those who suffer from DVT will ultimately develop post-thrombotic syndrome.[3] Post-thrombotic syndrome, caused by venous scarring, hypertension, and insufficiency, is characterized by swelling, pain, discoloration, and occasionally ulcerations in the affected extremity.[4] An estimated $7 to $10 billion is spent annually in the treatment of acute VTE and its complications.[5] VTE is a leading cause of disability-adjusted life-years,[6] and the mechanisms that drive it must be better understood so that targeted treatments and preventative strategies can be developed.

Venous thrombosis is driven by three categories of physiologic alterations known as Virchow's triad: stasis of blood flow, a state of hypercoagulability, and endothelial damage. A number of genetic and acquired conditions related to Virchow's triad increase the risk of DVT, such as deficiencies of antithrombin, protein C, or protein S; mutations in factor V Leiden or prothrombin; older age; obesity; prolonged immobility; pregnancy; cancer; oral contraceptive use; and smoking.[1] Although many of the clinical risk factors for DVT are well-established, the cellular and molecular mechanisms that drive venous thrombosis remain incompletely defined. A limited number of recently published studies suggest a role for receptor interacting protein kinase 3 (RIPK3) in thrombosis.[7,8]

Briefly, RIPK3 and its signaling partner receptor interacting protein kinase 1 (RIPK1) play a critical role in necroptosis, a form of regulated and inflammatory cell death distinct from apoptosis or necrosis. In the setting of an inflammatory stimulus, the presence of RIPK3 and RIPK1, and inhibitors of apoptosis, cells can be shunted down an inflammatory, necroptotic cell death pathway. This pathway culminates in the phosphorylation and oligomerization of mixed lineage domain like pseudokinase (MLKL), which interacts with the plasma membrane to cause a rapid loss of membrane integrity and subsequent release of proinflammatory intracellular contents.[9,10] RIPK3 is thought to play a role in cardiovascular diseases, not only by driving necroptosis of vascular cells, but also by promoting inflammation and pathologic coagulation.[9] Zhang et al[8] recently showed that RIPK3 plays a critical role in regulating platelet function in arterial thrombosis. RIPK3-deficient mice were noted to have prolonged bleeding times compared with wild-type littermates as well as prolonged vessel occlusion times in an in vivo model of arteriole thrombosis. RIPK3-deficient platelets demonstrated defects in aggregation and granule secretion in response to activating stimuli. In the only known study of necroptotic proteins in venous thrombosis, Nakazawa et al[7] showed that RIPK1 inhibition decreased thrombus size in the murine inferior vena cava (IVC) ligation model of venous thrombosis. Moreover, the authors found that RIPK1 inhibition and MLKL deficiency decreased the burden of procoagulant neutrophils extracellular traps (NETs) within thrombi. The role of RIPK3 in venous thrombosis has yet to be investigated directly.

This investigation sought to characterize the role of RIPK3 in venous thrombogenesis using murine models of DVT. The acute timepoints (0-48 hours) were selected because thrombus size peaks at 48 hours in the selected murine models of DVT. We found that, despite the accumulation of RIPK3 within the vessel wall and thrombus, deficiency or inhibition of RIPK3 failed to inhibit venous thrombogenesis at the 48-hour time point. Future investigations characterizing the role of RIPK3 in thrombus resolution and post-thrombotic vein wall remodeling will be of interest.

ARTICLE HIGHLIGHTS

- **Type of Research:** Mouse model
- **Key Findings:** The cell-death promoting protein receptor interacting protein kinase 3 (RIPK3) accumulates within the vein wall and thrombus in a mouse model of venous thrombosis, but deficiency or inhibition of RIPK3 fails to decrease thrombus size.
- **Take Home Message:** Although the absence of RIPK3 fails to decrease thrombus burden, further investigations are needed to determine whether or not local RIPK3 accumulation contributes to adverse post-thrombotic vein wall remodeling.

METHODS

Mice. All animal studies were performed with the approval of the Institute Animal Care and Use Committee at the University of Wisconsin—Madison. Eight- to 12-week-old male C57BL/6J mice (Jackson Laboratory, Bar Harbor, ME; Stock #000664), and *Ripk3*$^{-/-}$ and *Ripk3*$^{+/+}$ mice bred on a C57BL/6 background in house were used for all studies. Mice for individual studies were age and sex matched. Male mice were used as the gonadal vein anatomy of female mice increases variability in DVT models.[11] The *Ripk3* knockout (*Ripk3*$^{-/-}$) was a generous gift from Dr Dixit.[12] A total of 97 mice were used, 50 C57BL6, 23 *Ripk3*$^{+/+}$, and 24 *Ripk3*$^{-/-}$.

IVC ligation and stenosis surgery. Anesthesia was induced with 5% isoflurane, and anesthesia was maintained using 2.5% isoflurane in 100% oxygen thereafter.

A midline laparotomy was performed and the IVC was exposed performing a right medial visceral rotation.

For IVC ligation, back branches draining into the IVC between the renal and iliac veins were cauterized. Side branches were ligated with 7/0 polypropylene suture. A small window was made between the aorta and IVC immediately inferior to the insertion of the left renal vein, and the IVC was ligated at this location using 7/0 polypropylene suture. The sham surgery consisted of vessel dissection without suture placement or cautery.

For IVC stenosis, side branches were ligated with 7/0 polypropylene suture. A small window was made between the aorta and IVC immediately inferior to the insertion of the left renal vein. A 30G spacer needle was placed on the anterior aspect of the IVC, and 7/0 polypropylene was tied down around the IVC and spacer needle at this location. The needle was removed carefully, restoring approximately 10% residual flow through the IVC.

The intra-abdominal contents were returned and the abdomen was closed in a layered fashion. The mouse recovered under direct supervision. All mice were given a subcutaneous injection of slow-release buprenorphine (0.5 mg/kg) immediately before surgery, providing analgesia for 72 hours after surgery.

Propidium iodide injection. Two hours before euthanasia, an intraperitoneal injection of propidium iodide (PI) (P1470 Millipore Sigma, Burlington, MA) dissolved in phosphate-buffered saline was delivered to mice at a dose of 15 mg/kg body weight, as described by Wang et al.[13] Mice were monitored for adverse reactions between administration and euthanasia. All mice tolerated treatment well with 0% mortality. At time of euthanasia, mice were perfusion fixed (4% paraformaldehyde) and IVC/thrombus samples were harvested and embedded in optimal cutting temperature compound for frozen sectioning. We cut 6-μm-thick sections, counterstained them with DAPI (E19-100; GBI Labs, Bothell, WA) and an antibody against α-smooth muscle actin (α-SMA) (ab 8211, Abcam, Cambridge, UK; 1 ng/μL). Sections were visualized on a Nikon Confocal Microscope. PI-positive cells, as compared with total nucleated cells, within the vein wall and thrombus were quantified across three to six high-powered images (fewer images were used in sham sections owing to less wall distension).

Murine GSK'074 treatment. GSK'074 (0.93 mg/kg) was dissolved in 90:5:5 H_2O:dimethylsulfoxide:Cremophore EL and injected intraperitoneally into mice every 24 hours starting 24 hours before IVC ligation or sham surgery. This dose was selected based on prior studies from our group showing that daily intraperitoneal treatment with 0.93 mg/kg GSK'074 significantly attenuates abdominal aortic aneurysm formation in two mouse models of abdominal aortic aneurysm.[14] Control mice were injected with an equal volume of 90:5:5 H_2O:dimethylsulfoxide:Cremophore EL (referred to as solvent hereafter).

Tissue harvest. At the time of humane killing, mice were anesthetized with isoflurane and the IVC was exposed to allow for collection of the IVC and any associated thrombi. In a subset of mice, the IVC was skeletonized from surrounding structures, removed, and separated from any associated thrombus. The thrombus length was measured precisely by visualizing the thrombus under an operating microscope. Thrombus plus IVC weight was determined using a high precision scale. IVC and thrombus tissue were subsequently snap frozen in liquid nitrogen before being stored at −80°C until further processing. In a separate subset of mice, IVC, thrombus, and aorta were harvested en bloc at the level of the IVC ligature (superior boundary) and iliac veins (inferior boundary). Tissue samples were embedded in the optimal cutting temperature compound, frozen, and stored at −80°C until further processing by Western blot analysis.

Western blot. IVC and thrombus tissues were pulverized while frozen on liquid nitrogen and lysed using RIPA buffer containing protease and phosphatase inhibitors. Protein was quantified using the DC Protein Assay (Bio-Rad, Hercules, CA). An equal amount of protein was loaded per lane into a 10% bis-tris acrylamide gel. Membranes were blocked with 5% milk in Tween-Tris Buffered Saline before incubation with antibodies. Membrane-bound RIPK3 was detected using RIPK3 (D4G2A) rabbit monoclonal antibodies (mAb) (95702, Cell Signaling Technology, Danvers, MA); MLKL was detected using MLKL (D6W1K) rabbit mAb (33705, Cell Signaling Technology); glyceraldehyde 3-phosphate dehydrogenase was detected using glyceraldehyde 3-phosphate dehydrogenase (14C10) rabbit mAb (2118, Cell Signaling Technology). All primary antibodies were used at a 1:1000 dilution. Horseradish peroxidase-conjugated secondary antibodies against rabbit were used at 1:2000 dilution. All primary antibodies were diluted in Antibody Diluent (003118, ThermoFisher Scientific, Waltham, MA), and all secondary antibodies were diluted in 5% milk in Tween-Tris Buffered Saline.

Immunohistochemistry. Fresh frozen ICV/thrombus samples were cross-sectioned at a thickness of 6 μm. Sections were immunostained with the following primary antibodies: anti-CD31 (AF3628, R&D Systems, Minneapolis, MN; 1:40); anti-α-SMA (ab 8211, Abcam; 1:500); anti-RIPK3 (95702, Cell Signaling Technology, 1:100); anti pMLKL (phospho S345) (ab196436, Abcam, 1:100), anti-CD41 (MA5-16875, Invitrogen, Waltham, MA; 1:1000). Tissue samples were subsequently stained with AlexaFluor 488 and 594 antibodies. Sections were counterstained

with DAPI-containing mounting media (Fluorescent Mounting Medium with DAPI, GBI Labs, Cat No E19-100/E19-18). Images were acquired on a Nikon Confocal Microscope. Quantification was performed using Fiji/Image J software: images were subject to uniform color thresholds to identify stained regions of interest and were subsequently processed to be binary. Total region for analysis was mapped using the polygon selection tool, and percent area positive for the stain of interest was subsequently measured. Three to five high-powered fields were analyzed per mouse.

Terminal deoxynucleotidyl transferase dUTP nick end labeling staining. Terminal deoxynucleotidyl transferase dUTP nick end labeling (TUNEL) staining was performed on 6-μm IVC/thrombus fresh frozen sections using an In Situ Cell Death Detection Kit (Roche Holding AG, Basel, Switzerland; Cat No 12 156 792 910) according to manufacture instructions. Costaining with anti-α-SMA (ab 8211, Abcam; 1:500) was performed. Images were acquired on a Nikon Confocal Microscope. TUNEL positive cells, as compared with total nucleated cells, within the vein wall and thrombus were quantified across three to six high-powered images (fewer images were used in sham sections owing to less wall distension).

Statistic analyses. Results are reported as mean ± standard deviation if normally distributed or median ± interquartile range if not normally distributed. Statistical analysis was performed in GraphPad Prism Software Version 9 (GraphPad Software Inc, La Jolla, CA) using an unpaired Student *t*-test for normally distributed continuous variables, the Mann-Whitney *t*-test for non-normally distributed continuous variables, and one-way analysis of variance with Dunnett's multiple comparisons test. Simple linear regression was used for correlative analyses. A *P* value of less than .05 was considered statistically significant.

RESULTS

RIPK3 accumulates in both the vein wall and thrombus during thrombogenesis. To determine whether or not RIPK3 accumulates in the local thrombotic environment during thrombogenesis, a time course was performed analyzing vein wall and thrombus constituents during the acute phase of DVT (0-48 hours after IVC ligation). IVC and associated thrombus samples were collected from mice at 0, 6, 24, and 48 hours after IVC ligation. Thrombus weight gradually increased as expected across all timepoints (Fig 1, *A*). Within the thrombus, RIPK3 was detectable across all thrombus-bearing timepoints (6, 24, and 48 hours), but seemed be most abundant at earlier timepoints (6, >24 and >48 hours) (Fig 1, *B*). A strikingly different pattern appeared within vein wall specimens. At 0 hours (baseline), RIPK3 was barely detectable in vein wall specimens. RIPK3 accumulation gradually increased from 6 to 48 hours (Fig 1, *C* and *D*). A significant, positive correlation was found between RIPK3 abundance and thrombus weight across all samples (Fig 1, *E*). Although total MLKL, a marker of necroptosis, was detectable within thrombus samples across each timepoint (Fig 1, *B*), total MLKL was nearly undetectable across all timepoints within vein wall specimens, despite a high RIPK3 burden (Fig 1, *C*).

RIPK3 accumulates within smooth muscle and endothelial cells within the vein wall. To determine where RIPK3 was accumulating within the vein wall, dual immunofluorescent staining was performed for RIPK3 and vascular and immune cell populations in tissue sections harvested 48 hours after IVC ligation or sham surgery. At 48 hours after IVC ligation, the influx of neutrophils into the vein wall is high. Given existing literature suggesting that the necroptotic and NETosis pathways are closely linked,[7] we first investigated whether or not RIPK3 localizes to invading neutrophils ($Ly6G^+$) within both the vein wall and thrombus. As expected, a high burden of neutrophils within the thrombus and vein wall were appreciated (Supplementary Fig 1). Although Ly6G-positive cells localized to areas adjacent to RIPK3-positive tissue, both within the thrombus and vein wall, the RIPK3 burden within Ly6G-positive cells was low in the thrombus and vein wall (Supplementary Fig 1).

Within the vessel wall, RIPK3 highly colocalized to both smooth muscle cells (α-SMA^+) and endothelial cells ($CD31/PECAM^+$) (Fig 2, *A-E*). Although there was a trend toward a higher density of RIPK3 staining in smooth muscle cells compared with endothelial cells, this failed to reach statistical significance (RIPK3-positive area, 32.4% vs 23.4%; $P = .26$) (Supplementary Fig 2). Consistent with our Western blot results, RIPK3 was detectable but in very low levels in vein wall specimens from non-DVT-bearing (sham-operated) mice. More broadly, at 48 hours after IVC ligation, RIPK3 staining was greater in the vessel wall compared with the thrombus (Fig 2, *C*).

Markers of necroptosis and cell death are low in the vein wall, despite a high RIPK3 burden. Phosphorylation of MLKL on serine 345 by RIPK3 is a necessary signaling step for cell necroptosis. We performed dual immunofluorescent staining for phosphorylated MLKL (pMLKL) and smooth muscle cell (α-SMA^+) and endothelial markers (CD31/PECAM) on tissue specimens from mice 48 hours after IVC ligation or sham surgery (Fig 3, *A* and *B*). In all specimens, pMLKL burden was greater in the thrombus compared with the vessel wall (Fig 3, *A-C*). Regions of pMLKL/α-SMA^+ and pMLKL/CD31 copositivity were minimal. pMLKL was nearly undetectable in sham vessel wall specimens. Various regions within the thrombus that stained positively for pMLKL also stained positively for

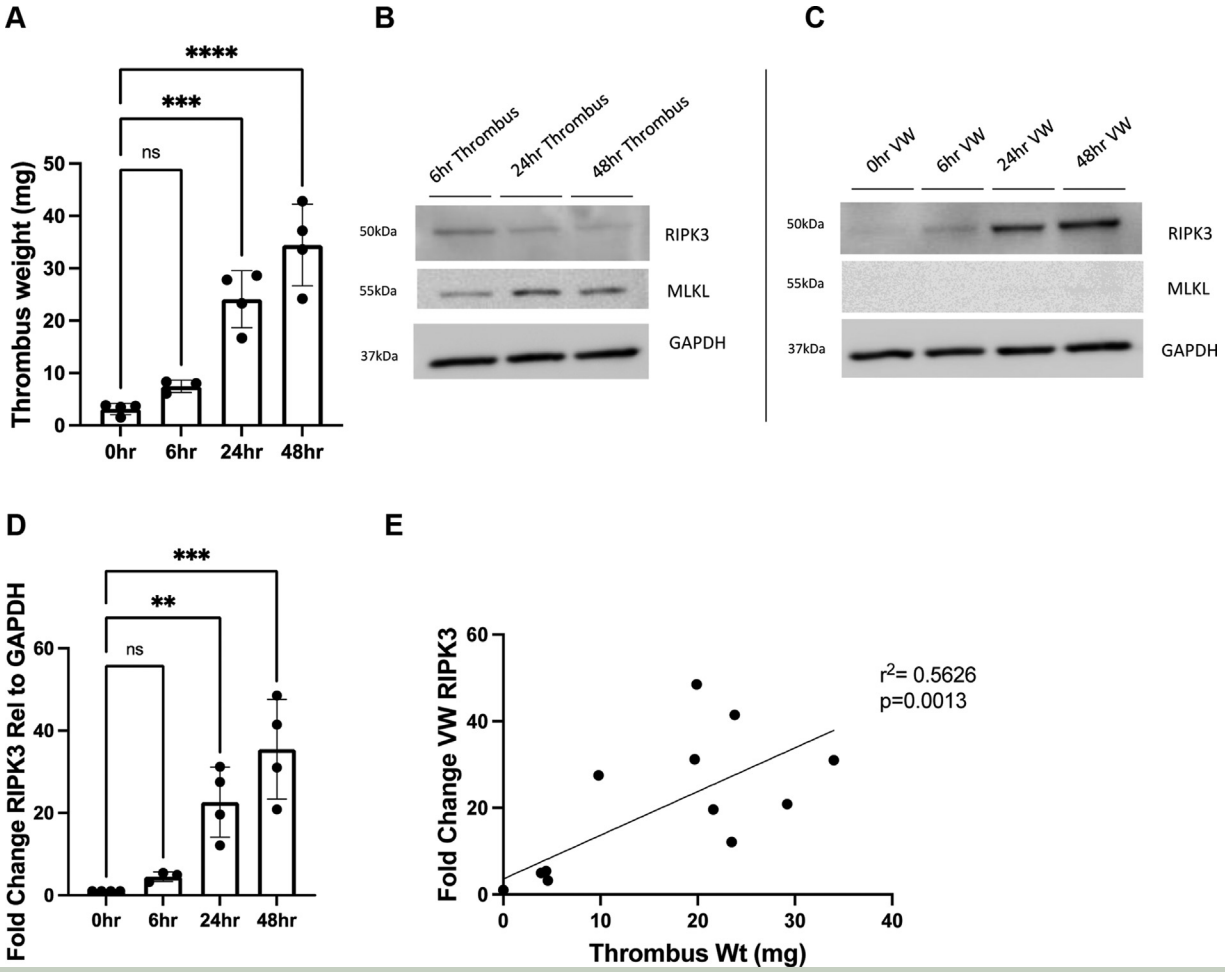

Fig 1. Receptor interacting protein kinase 3 (RIPK3) accumulates in the vein wall during thrombogenesis. **A,** Thrombus weight (thrombus plus associated inferior vena cava [IVC] weight) was measured at 0, 6, 24, and 48 hours after IVC ligation (n = 15 total). **B,** Representative Western blot for RIPK3 and mixed lineage kinase domain like pseudokinase (MLKL) in thrombus specimens from mice 6, 24, and 48 hours after IVC ligation. Glyceraldehyde 3-phosphate dehydrogenase (*GAPDH*) was used as a loading control. **C,** Representative Western blot for RIPK3 and MLKL in vein wall specimens from mice 0, 6, 24, and 48 hours after IVC ligation. GAPDH was used as a loading control. **D,** Quantification of RIPK3 Western blots performed on vein wall specimens 0, 6, 24, and 48 hours after IVC ligation. Fold change in RIPK3 relative to GAPDH and compared with 0hr timepoint shown. **E,** Correlation between fold change in RIPK3 within the vein wall (*VW*) **(D)** and thrombus weight **(A)**. Unpaired Student *t*-test was performed in **(A** and **D)**. Pearson's correlation coefficient shown in **(E)**. $^{**}P < .01$; $^{***}P < .001$.

CD31. We suspected these regions may be platelet rich, because CD31 can also be found on the surface of platelets. Platelet marker CD41 and pMLKL dual staining of 48-hour thrombus specimens did reveal colocalization of pMLKL and CD41 within the thrombus periphery (Supplementary Fig 3).

High levels of RIPK3 can drive cell death through necrotic (necroptosis) and non-necrotic (apoptosis) pathways.[15] We next investigated whether or not high RIPK3 within the vessel wall is associated with necrotic or apoptotic vein wall cell death. PI, a DNA intercalating agent that only enters necrotic cells, was delivered to mice 46 hours after IVC ligation or sham operation. At 48 hours after IVC ligation, IVC/thrombus tissue was collected, sectioned, counterstained with α-SMA and DAPI for vein wall and nuclear localization, and imaged. PI-positive cells were abundant within the periphery of 48-hour thrombi, whereas PI-positive cells within the vein wall were sparse (Fig 4, *A*). PI-positive cells were nearly undetectable in sham-operated vein wall specimens (Fig 4, *A* and *C*). TUNEL staining was performed on tissue collected from non-PI-treated, 48-hour DVT-bearing or sham-operated mice to evaluate apoptotic cell burden. Although abundant TUNEL-positive cells were seen within the thrombus itself, relatively few apoptotic cells were seen within the DVT-bearing vein

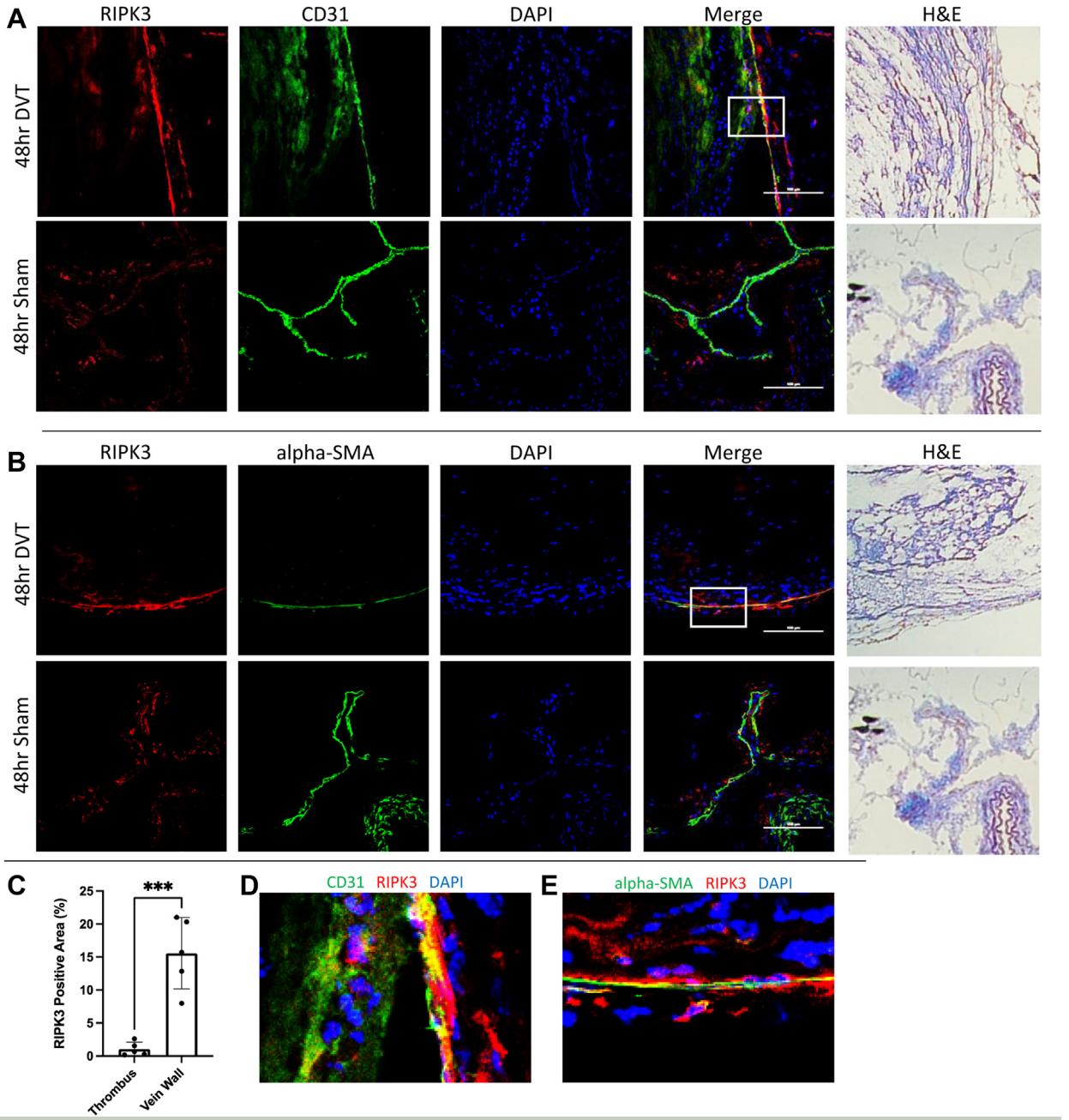

Fig 2. Receptor interacting protein kinase 3 (RIPK3) localizes to the intima and media in the vein wall during thrombogenesis. C57BL6/J mice were subjected to inferior vena cava (IVC) ligation (n = 5) or sham surgery (n = 3). At 48 hours after surgery, the IVC and thrombus tissues were collected and cross-sectioned. **A,** Anti-RIPK3 *(red)* and CD31/PECAM *(green)* were used to identify RIPK3 burden in endothelial cells in 48-hour deep vein thrombosis (*DVT*) and sham sections. The white box is shown magnified in **(D)**. **B,** Anti-RIPK3 *(red)* and anti-alpha smooth muscle actin (α-SMA) *(green)* were used to identify RIPK3 burden in smooth muscle cells in 48-hour DVT and sham sections. The white box shown magnified in **(E)**. DAPI was used to stain nuclei in **(A** and **B)**. **C,** Quantification of RIPK3 positively stained area within thrombus and vein wall regions. **D,** Magnified view of the vein wall/thrombus interface shown in **(A)**. **E,** Magnified view of the vein wall/thrombus interface shown in **(B)**. Scale bar, 100 μm. Data are presented as mean ± standard deviation. The unpaired Student *t* test was performed in **(C)**. ***$P < .001$. *H&E*, hematoxylin and eosin.

wall, primarily localizing to the adventitia and beyond (Fig 4, *B*). TUNEL-positive cells, much like PI-positive cells, were nearly undetectable in sham-operated vein wall specimens (Fig 4, *B* and *D*).

Deficiency and inhibition of RIPK3 do not alter thrombus weight. Given the robust accumulation of RIPK3 within the vessel wall and detectable RIPK3/MLKL within the thrombus, we hypothesized that

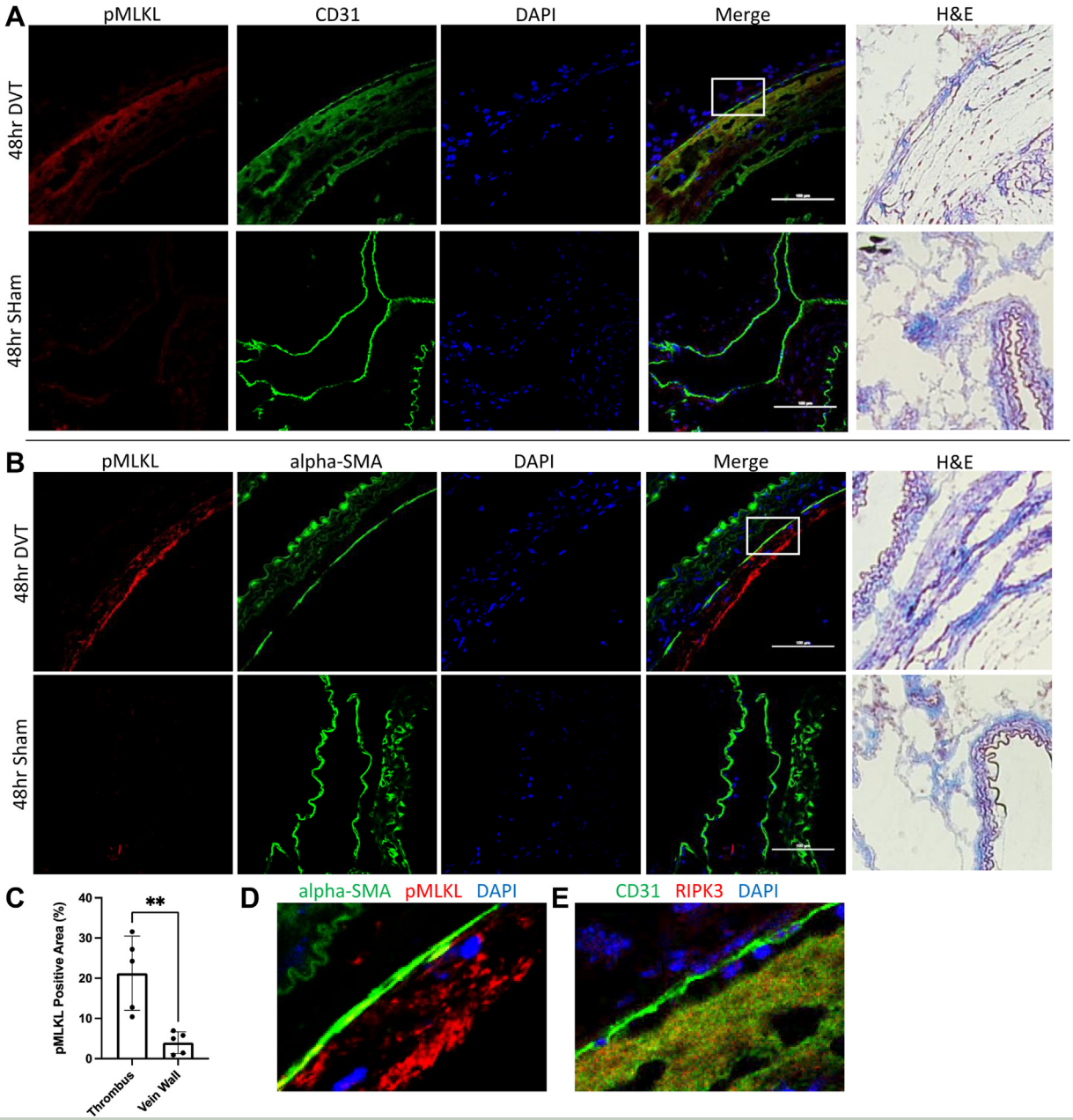

Fig 3. Phosphorylated mixed lineage kinase domain like pseudokinase (pMLKL) localizes primarily to the thrombus as opposed to vein wall during thrombogenesis. **A,** Anti-pMLKL *(red)* and CD31/PECAM *(green)* were used to identify pMLKL burden in endothelial cells in 48 hour deep vein thrombosis (DVT) (n = 5) and sham (n = 3) sections. The white box is shown magnified in **(D)**. **B,** Anti-pMLKL *(red)* and anti-alpha smooth muscle actin (α-SMA) *(green)* were used to identify pMLKL burden in smooth muscle cells in 48-hour DVT and sham sections. The white box is shown magnified in **(E)**. DAPI was used to stain nuclei in **(A** and **B)**. **C,** Quantification of pMLKL positively stained area within thrombus and vein wall regions. **D,** Magnified view of the vein wall/thrombus interface shown in **(A)**. **E,** Magnified view of the vein wall/thrombus interface shown in **(B)**. Scale bar, 100 μm. Data are presented as mean ± standard deviation. The unpaired Student *t*-test was performed in **(C)**. ** $P < .01$. *H&E*, hematoxylin and eosin.

RIPK3 may play an important role in thrombogenesis. To test this hypothesis, we performed the IVC ligation model in wild-type (*Ripk3*$^{+/+}$) and RIPK3-deficient (*Ripk3*$^{-/-}$) mice and evaluated thrombus burden at 48 hours after operation. Thrombus weight was not significantly different between wild-type and RIPK3-deficient mice among all mice (Fig 5, *A*) or only those that formed thrombi (Fig 5, *B*). NET burden, as determined by cocitrullinated H3 and Ly6G staining, seemed to be similar both within the body of the thrombus and

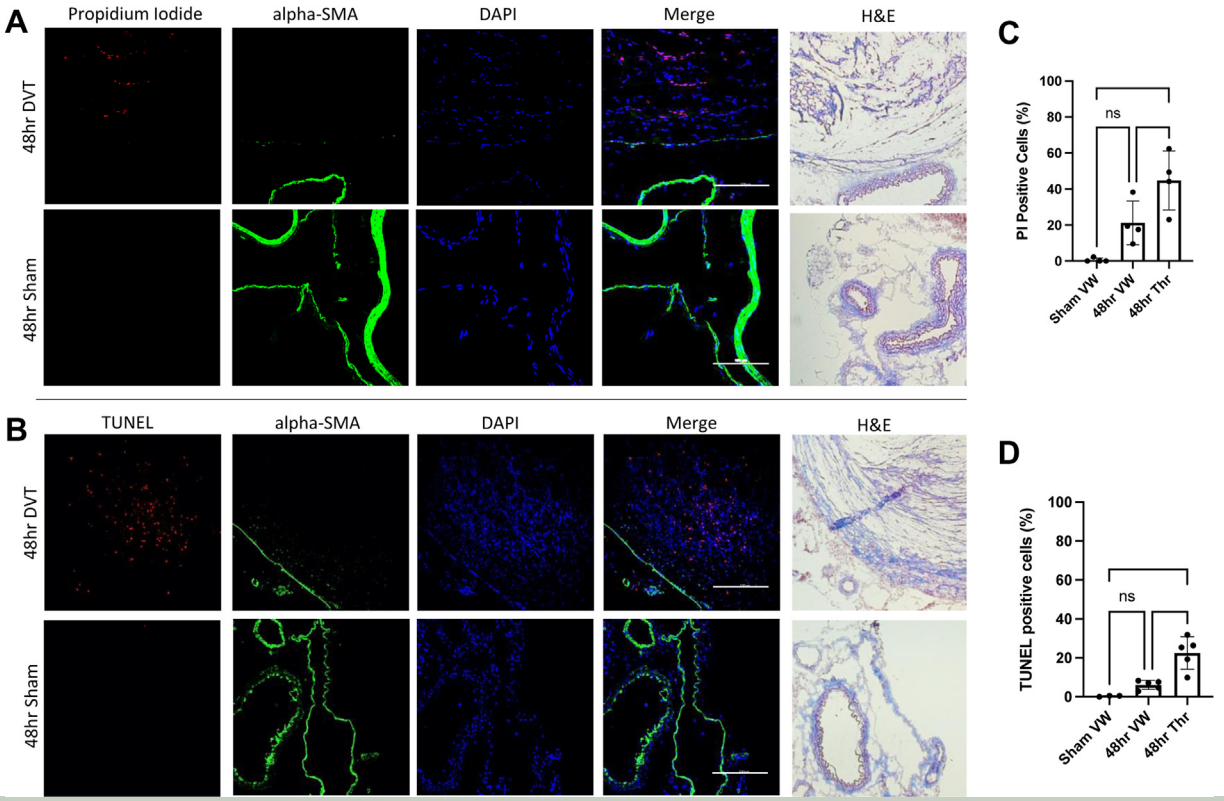

Fig 4. Low cell death burden is detected in the vein wall 48 hours after inferior vena cava (IVC) ligation. C57BL6/J mice were subjected to IVC ligation (n = 4) or sham (n = 3) surgery. At 46 hours after surgery, a subset of mice were treated with propidium iodide (*PI*) by intraperitoneal injection. A separate subset of mice underwent no treatment. At 48 hours after surgery, IVC and thrombus tissues were collected and cross sectioned. **A,** PI (red) positivity in the vein wall and thrombus, with anti-alpha smooth muscle actin (α-SMA) *(green)* stained for orientation purposes. **B,** Terminal deoxynucleotidyl transferase dUTP nick end labeling (*TUNEL*) *(red)* staining in the vein wall and thrombus, with anti-α-SMA (green) stained for orientation purposes. **C,** PI-positive cells, shown as a total percentage of nucleated cells, in the vein wall and thrombus. **D,** TUNEL-positive cells, shown as a total percentage of nucleated cells, in the vein wall and thrombus. Scale bar, 100 μm. Data are presented as mean ± standard deviation. One-way analysis of variance was performed in **(C** and **D)**. * $P < .05$, ** $P < .01$, *** $P < .001$. *H&E*, hematoxylin and eosin; *VW*, vein wall.

the adjacent vein wall in wild-type and RIPK3-deficient mice (Fig 5, *C* and *D*). No differences in cocitrullinated H3 burden were detected in 48-hour thrombus or vein wall specimens from wild-type and RIPK3-deficient mice by Western blot analysis (Fig 5, *E-H*). To determine if our results were specific to the IVC ligation model, we performed the IVC stenosis model in wild-type and RIPK3-deficient mice and evaluated thrombus weight/length at 48 hours after operation. Thrombus weight and length were not significantly different between wild-type and RIPK3-deficient mice (Supplementary Fig 4, *A* and *B*). Exclusion of mice that failed to form thrombi did not reveal a significant difference in thrombus weight or length (Fig 4, *C* and *D*).

To exclude the potential influence of embryonic gene deletion, we investigated the effect of pharmacological inhibition of RIPK3 in the IVC ligation model. Because currently no targeted RIPK3 inhibitors exist with acceptable toxicity profiles, a dual RIPK1/3 (GSK2593074A [GSK'074])[14] inhibitor was used. C57BL6/J mice were treated with GSK'074 (0.93 mg/kg) or solvent, starting 24 hours before IVC ligation or sham surgery. Doses were thereafter administered every 24 hours until tissue collection (48 hours after operation). GSK'074 was well-tolerated as compared with solvent (Fig 6, *A*). One of seven mice in the solvent group failed to form a DVT after IVC ligation as compared with two of six mice in the GSK'074 group, a nonstatistically significant difference (Fig 6, *B*). Thrombus weight and length were not significantly different at 48 hours after IVC ligation between GSK'074- and solvent-treated mice (Fig 6, *C* and *D*).

DISCUSSION

Although the existing literature is limited, our results are somewhat unexpected in light of two studies showing a role for necroptotic proteins (eg, RIPK1, RIPK3, and MLKL) in arterial and venous thrombosis. Briefly, Zhang et al[8] showed that mice deficient in

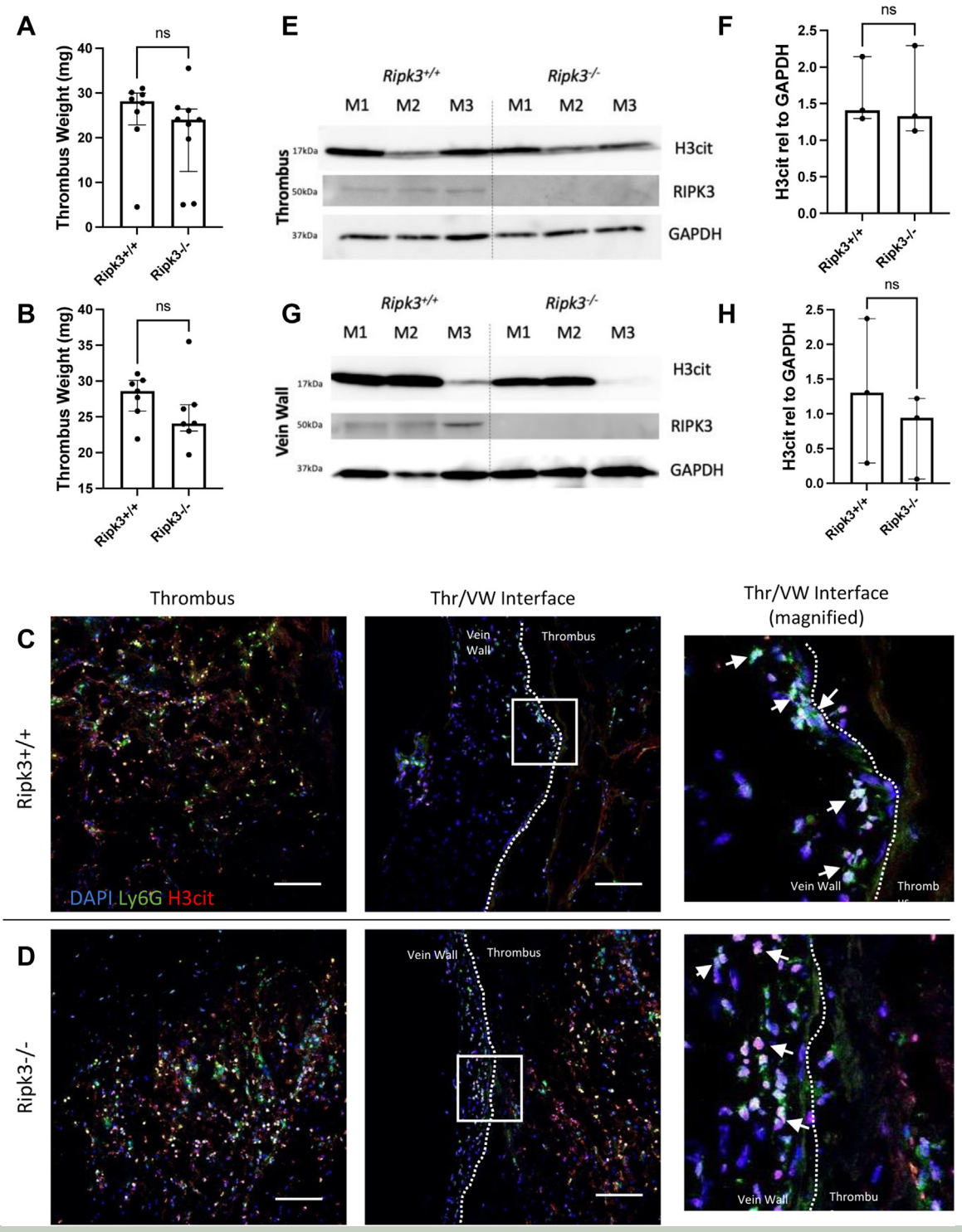

Fig 5. Receptor interacting protein kinase 3 (RIPK3) deficiency does not alter thrombus (*Thr*) size or neutrophils extracellular trap (NET) burden 48 hours after inferior vena cava (IVC) ligation. Wild-type (*WT*) (*Ripk3*$^{+/+}$) and RIPK3-deficient (*Ripk3*$^{-/-}$) mice underwent IVC ligation followed by tissue collection 48 hours after surgery (WT n = 8, knockout [KO] n = 9). Thrombus weight (thrombus plus associated IVC weight) in total mice **(A)** and in only in those mice that formed thrombi **(B)** were compared between the two genotypes. A separate subset of mice underwent tissue harvest for histologic examination (WT n = 3, KO n = 3). Staining for NETs (cocitrullinated H3 [*H3cit*] in red, Ly6G in green) was performed on WT **(C)** and *Ripk3* gene-deficient **(D)** IVC/thrombus sections (longitudinal). Areas of exclusive thrombus tissue (left) and the thrombus/vein wall (*VW*) interface were examined (center). Vein wall/thrombus interface shown with white dotted line. Region within white box is shown magnified in the rightmost panel. (E-H) Representative Western blots and quantifications for H3cit and RIPK3 in thrombus speciments **(E** and **F)** and the vein wall **(G** and **H)** from mice 48 hours after IVC ligration. GAPGH was used as a

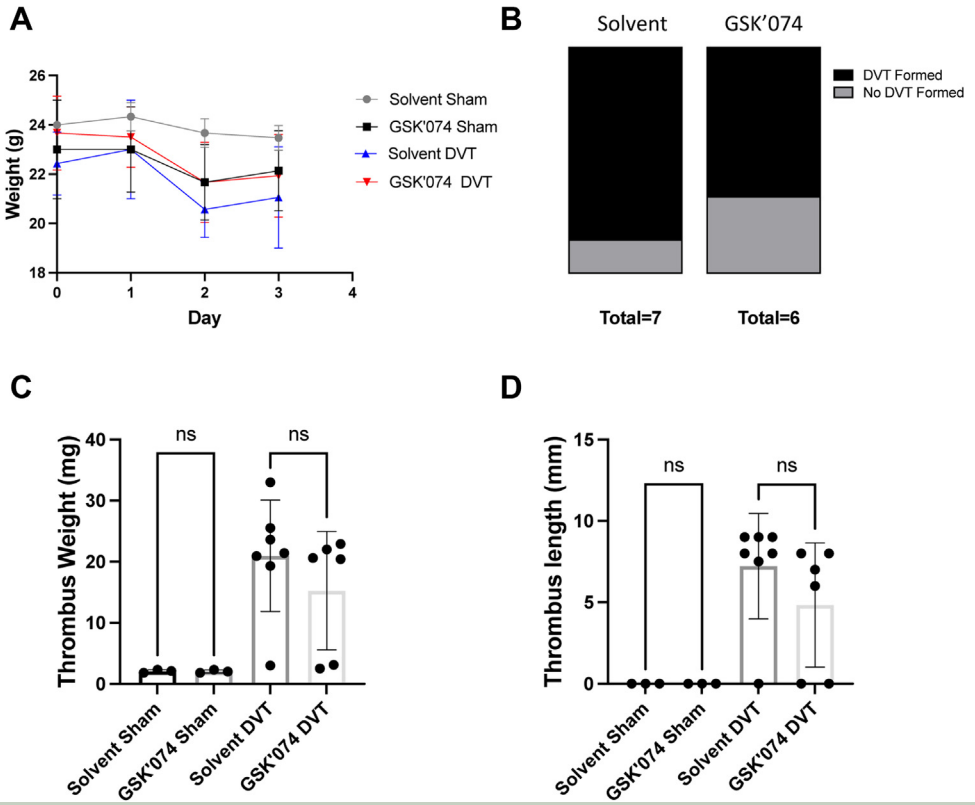

Fig 6. Perioperative receptor interacting protein kinase 3 (RIPK3)/RIPK1 inhibition does not alter acute thrombus incidence or size in the inferior vena cava (IVC) ligation model. C57BL6/J mice were treated with GSK'074 (0.93 mg/kg, intraperitoneal injection) (n = 10) or solvent (n = 10) starting 24 hours before surgery. Dosing was repeated every 24 hours until time of tissue collection, 48 hours post operation. **A,** Body weights were monitored daily to assess drug tolerance. **B-D,** The incidence of thrombus formation as well as thrombus weight and length were compared among groups. Data are presented as mean ± standard deviation. Two-way analysis of variance was performed in **(A)**. Fischer's exact test was performed in **(B)**. One-way analysis of variance was performed in **(C** and **D)**. *DVT*, Deep vein thrombosis.

RIPK3 exhibit decreased mesenteric arteriole thrombosis, and that RIPK3 promotes platelet activation and subsequent arterial clot formation. In a study investigating the role of MLKL in venous thrombosis, Nakazawa et al[7] showed that mice deficient in MLKL or treated with a RIPK1 inhibitor (necrostatin-1s) develop smaller thrombi with significantly lower burdens of NETs after IVC ligation compared with wild-type littermates or control-treated mice respectively. Similar to Nakazawa et al, we found that RIPK3 and pMLKL can be detected within murine thrombi at early timepoints after IVC ligation. However, we did not detect a difference in thrombus size between mice lacking RIPK3 and their wild-type littermates, or between mice treated with a dual RIPK1/RIPK3 inhibitor (GSK'074) and solvent-treated mice. Nakazawa et al had a slightly different dosing scheme for necrostatin-1s-treated mice compared with our GSK'074 treatment (1 hour before surgery treatment, as opposed to 24 hours before, followed by immediate postoperative and 24-hour postoperative treatments), which may be a contributing factor to the differences observed. Although Nakazawa et al never directly investigated the role of RIPK3 in venous thrombosis, instead focusing on RIPK1 and MLKL, the codependence between RIPK1 and RIPK3 in the necroptotic pathway, and fact that RIPK3 is the only known activator of MLKL, make our findings unexpected. It is possible that subtle differences in the execution of the mouse models of venous thrombosis may contribute to the differences in our findings. Nakazawa et al described performing IVC ligation without side or back branch interruption, a variation between the described stasis and stenosis murine models of DVT. We performed the

loading control. Scale bar, 100 μm. Data are presented as median ± interquartile range. H3cit/Ly6G copositive cells (NETs). Mann-Whitney U *t*-test was performed in **(A**, **B**, **F**, and **H)**. *GADPH*, Glyceraldehyde 3-phosphate dehydrogenase.

majority of our experiments using the commonly performed stasis model of DVT, which involves not only IVC ligation, but also back and side branch interruption. We did, however, also assess thrombus formation and size in the IVC stenosis model—a model perhaps closer to that described by Nakazawa et al[7,11]—and similarly found no difference in thrombus size between wild-type and RIPK3-deficient mice.

Multiple processes or factors in the DVT group could contribute to the elevation of RIPK3, including the physical trauma imposed by venous ligation and the subsequent changes in blood flow, hypoxia, oxidative stress, and/or inflammation. As the thrombus grows, it stretches the vein wall and worsens hypoxia. It is also possible that cells and factors within the blood clots such as neutrophils, NETs, and clotting factors stimulate the expression of RIPK3 by endothelial and smooth muscle cells.

The accumulation of RIPK3 within the DVT-bearing vein wall and its disassociation with markers of cell death and NETosis are interesting, filling a knowledge gap in the DVT literature. Of note, only thrombus, as opposed to thrombus and vein wall samples, were investigated in the study performed by Nakazawa et al.[7] Although nearly undetectable in naive and sham-operated vein walls, RIPK3 substantially increased in the vein wall from 0 to 48 hours after IVC ligation. Compared with the adjacent thrombus, the relative burden of RIPK3 within the vein wall was significantly greater, primarily localizing to endothelial and smooth muscle cells. Despite a high burden of RIPK3, and unlike in the thrombus, pMLKL and downstream markers of cell death were present in relatively low levels in the vein wall. Prior studies from our group have demonstrated that vascular smooth muscle cells are capable of undergoing RIPK3-mediated necroptosis in vitro and in mouse models of aortic aneurysm.[13,14] The insignificant presence of cell death markers despite of high expression of RIPK3 within the vein wall is intriguing. It is possible that cell death occurs outside of the 48-hour timepoint examined. Although we intentionally only investigated timepoints representing the acute thrombogenic period for this initial study, future studies should interrogate downstream markers of necroptosis at timepoints beyond 48 hours after IVC ligation. Alternatively, cells in the vein wall may be adapted to a low oxygen environment and more resistant to necroptosis than their arterial counterparts. The low protein abundance of MLKL in the vein wall at the examined time points may explain, in part, the lack of necroptosis. RIPK1-mediated RIPK3 phosphorylation is critical for the onset of necroptosis[9]; however, we were unable to find an antibody that reliably detects phosphorylated RIPK3 in mouse veins. It is possible that the primary role of RIPK3 in the vein wall is in regulation of non-necroptotic process, such as inflammation or fibrosis. In support of this speculation, several studies have shown that RIPK3 plays an important role in kidney tissue fibrosis.[15-18] Vascular fibrosis is an essential component of the adverse post-thrombotic vein wall remodeling that contributes to post-thrombotic syndrome.[4] Future studies comparing post-thrombotic vein wall remodeling in wild-type and RIPK3-deficient mice would be worthwhile to pursue.[19]

This study is not without limitations. This study primarily relied on the IVC ligation (stasis) model of DVT, and no individual mouse model of venous thrombosis captures all the elements of thrombus formation that occur in humans affected by DVT. We did, however, validate our primary finding that DVT size is not different in wild-type and RIPK3-deficient mice in the IVC stenosis (flow) model of DVT, and further investigations using the stenosis model were not pursued given the lack of difference between the two sets of mice. Future studies using alternative flow-preserving models of DVT, such as the electrolytic injury model, would be of interest to use in studying the role of RIPK3 in DVT. Furthermore, a select number of acute timepoints were examined up to 48 hours after DVT induction. Studies examining the role of RIPK3 in thrombus resolution and vein wall remodeling across hyperacute (eg, 3-6 hours), subacute (eg, 2-8 days), and chronic (eg, >8 days) timepoints should be performed in the future. Given the impressive burden of RIPK3 that accumulates within the vessel wall during thrombogenesis, it seems unlikely that RIPK3 is purely a bystander in this disease process.

CONCLUSIONS

In conclusion, RIPK3 accumulates within both the vein wall and thrombus during thrombogenesis, although its absence or inhibition fails to reduce thrombus size in the murine IVC ligation and IVC stenosis models of DVT. The presence of downstream markers of necroptosis and cell death within the thrombus, but not the vein wall, is of great interest and worthy of further investigation.

AUTHOR CONTRIBUTIONS

Conception and design: ED, MK, TZ, HY, PH, BL
Analysis and interpretation: ED, CL, PH, BL
Data collection: ED, MK, TZ, HY, AS
Writing the article: ED, MK, TZ, HY, AS, CL, PH, BL
Critical revision of the article: ED, PH, BL
Final approval of the article: ED, MK, TZ, HY, AS, CL, PH, BL
Statistical analysis: ED
Obtained funding: ED, TZ, BL
Overall responsibility: BL

REFERENCES

1. Beckman MG, Hooper WC, Critchley SE, Ortel TL. Venous thromboembolism: a public health concern. Am J Prev Med 2010;38(4 Suppl): S495-501.
2. Raskob GE, Silverstein R, Bratzler DW, Heit JA, White RH. Surveillance for deep vein thrombosis and pulmonary embolism:

recommendations from a national workshop. Am J Prev Med 2010;38(4 Suppl):S502-9.
3. Galanaud JP, Monreal M, Kahn SR. Epidemiology of the post-thrombotic syndrome. Thromb Res 2018;164:100-9.
4. Kahn SR. The post-thrombotic syndrome. Hematology 2016;2016:413-8.
5. Grosse SD, Nelson RE, Nyarko KA, Richardson LC, Raskob GE. The economic burden of incident venous thromboembolism in the United States: a review of estimated attributable healthcare costs. Thromb Res 2016;137:3-10.
6. Thrombosis: a major contributor to the global disease burden. J Thromb Haemost 2014;12:1580-90.
7. Nakazawa D, Desai J, Steiger S, Müller S, Devarapu SK, Mulay SR, et al. Activated platelets induce MLKL-driven neutrophil necroptosis and release of neutrophil extracellular traps in venous thrombosis. Cell Death Discov 2018;4:6.
8. Zhang Y, Zhang J, Yan R, Tian J, Zhang Y, Zhang J, et al. Receptor-interacting protein kinase 3 promotes platelet activation and thrombosis. Proc Natl Acad Sci U S A 2017;114:2964-9.
9. Cho YS, Challa S, Moquin D, Genga R, Ray TD, Guildford M, et al. Phosphorylation-driven assembly of the RIP1-RIP3 complex regulates programmed necrosis and virus-induced inflammation. Cell 2009;137:1112-23.
10. Gautheron J, Vucur M, Reisinger F, Cardenas DV, Roderburg C, Koppe C, et al. A positive feedback loop between RIP3 and JNK controls non-alcoholic steatohepatitis. EMBO Mol Med 2014;6:1062-74.
11. Diaz JA, Saha P, Cooley B, Palmer OR, Grover SP, Mackman N, et al. Choosing a mouse model of venous thrombosis. Arterioscler Thromb Vasc Biol 2019;39:311-8.
12. Newton K, Sun X, Dixit VM. Kinase RIP3 is dispensable for normal NF-kappa Bs, signaling by the B-cell and T-cell receptors, tumor necrosis factor receptor 1, and Toll-like receptors 2 and 4. Mol Cel Biol 2004;24:1464-9.
13. Wang Q, Liu Z, Ren J, Morgan S, Assa C, Liu B. Receptor-interacting protein kinase 3 contributes to abdominal aortic aneurysms via smooth muscle cell necrosis and inflammation. Circ Res 2015;116:600-11.
14. Zhou T, Wang Q, Phan N, Ren J, Yang H, Feldman CC, et al. Identification of a novel class of RIP1/RIP3 dual inhibitors that impede cell death and inflammation in mouse abdominal aortic aneurysm models. Cell Death Dis 2019;10:226.
15. Orozco S, Oberst A. RIPK3 in cell death and inflammation: the good, the bad, and the ugly. Immunol Rev 2017;277:102-12.
16. Imamura M, Moon JS, Chung KP, Nakahira K, Muthukumar T, Shingarev R, et al. RIPK3 promotes kidney fibrosis via AKT-dependent ATP citrate lyase. JCI Insight 2018;3.
17. Qiao S, Hong L, Zhu Y, Zha J, Wang A, Qiu J, et al. RIPK1-RIPK3 mediates myocardial fibrosis in type 2 diabetes mellitus by impairing autophagic flux of cardiac fibroblasts. Cel Death Dis 2022;13:147.
18. Shi Y, Huang C, Zhao Y, Cao Q, Yi H, Chen X, et al. RIPK3 blockade attenuates tubulointerstitial fibrosis in a mouse model of diabetic nephropathy. Sci Rep 2020;10:10458.
19. Henke PK, Mitsuya M, Luke CE, Elfline MA, Baldwin JF, Deatrick KB, et al. Toll-like receptor 9 signaling is critical for early experimental deep vein thrombosis resolution. Arterioscler Thromb Vasc Biol 2011;31:43-9.

Submitted Jun 25, 2022; accepted Sep 19, 2022.

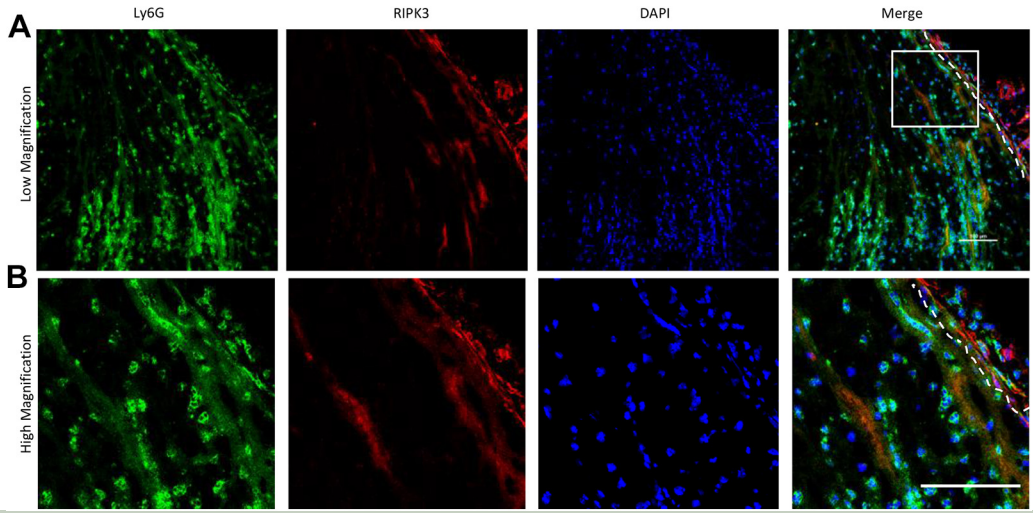

Supplementary Fig 1. Receptor interacting protein kinase 3 (RIPK3) burden in neutrophils is low in acute deep vein thrombosis (DVT). C57BL6/J mice were subjected to inferior vena cava (IVC) ligation. At 48 hours after surgery, IVC and thrombus tissue was collected and cross-sectioned. **A,** Anti-Ly6G *(green)* and RIPK3 *(red)* were used to identify RIPK3 burden in neutrophils in DVT sections (n = 5). Region encompassed by a white box is shown magnified in **(B)**. Vein wall (VW)/thrombus interface is indicated with white dotted line. Scale bar, 100 μm.

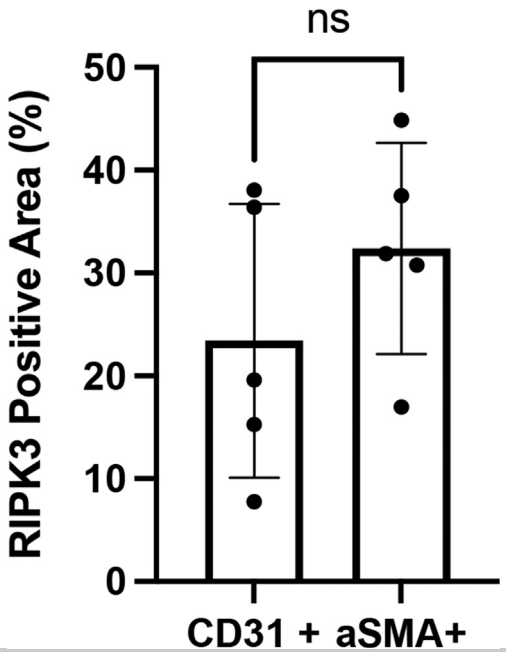

Supplementary Fig 2. Receptor interacting protein kinase 3 (RIPK3) abundance does not differ between endothelial and smooth muscle cells in acute deep vein thrombosis (DVT). RIPK3 positive area was quantified within CD31 positive (endothelial) and alpha-smooth muscle actin (α-*SMC*)-positive regions of the vessel wall 48 hours after inferior vena cava (IVC) ligation (representative images shown in Fig 2, n = 5 per group). An unpaired Student *t*-test was performed.

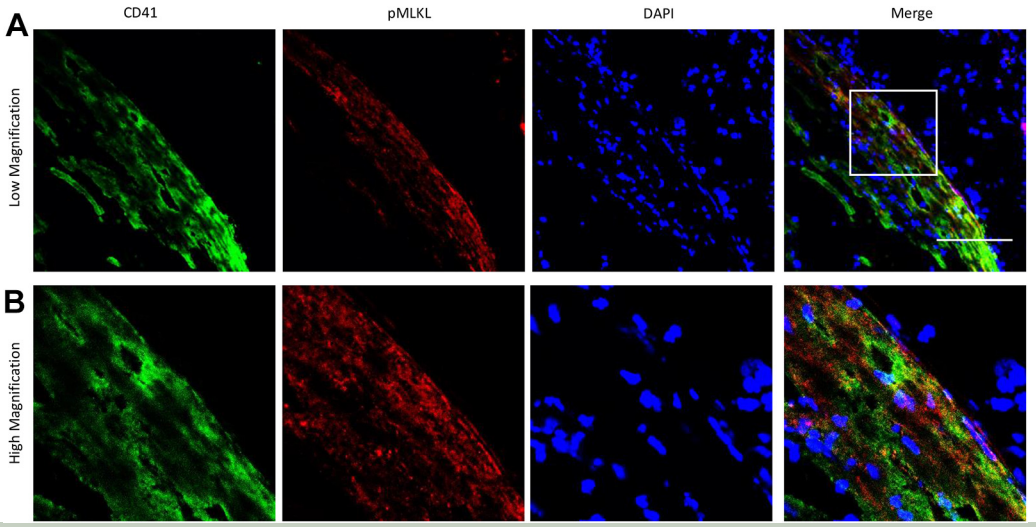

Supplementary Fig 3. Phosphorylated mixed lineage kinase domain like pseudokinase (pMLKL) colocalizes to platelet rich regions of thrombi. 48 hours after surgery, IVC and thrombus tissues were collected and cross-sectioned. **A,** Anti-CD41 *(green)* and pMLKL *(red)* were used to identify platelet and pMLKL-rich regions within acute thrombus sections (n = 5). Region encompassed by the white box is shown magnified in **(B)**. Scale bar, 100 μm.

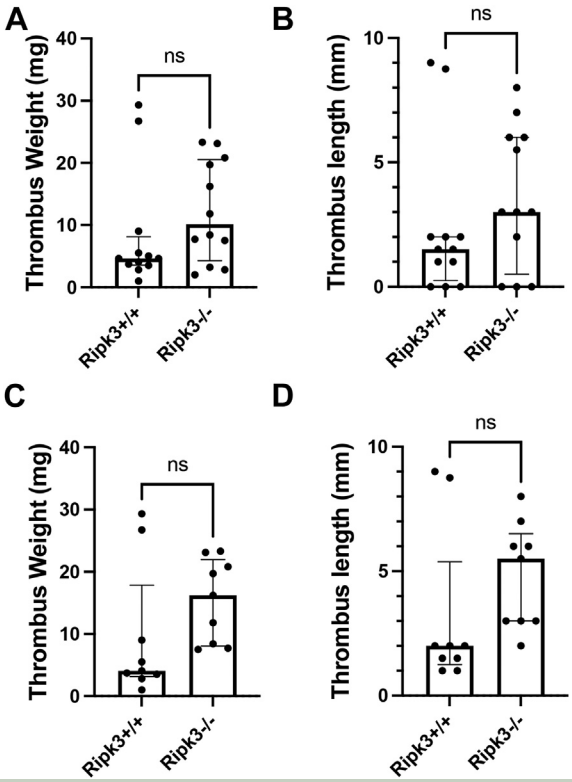

Supplementary Fig 4. Receptor interacting protein kinase 3 (RIPK3) deficiency does not alter thrombus size after inferior vena cava (IVC) stenosis. Wild-type (WT) (*Ripk3*$^{+/+}$) and RIPK3-deficient (*Ripk3*$^{-/-}$) mice underwent IVC stenosis followed by tissue collection 48 hours after surgery (WT n = 12, KO n = 12). Thrombus weight **(A)** and length **(B)** in all mice, and in mice that formed thrombi **(C** and **D)** were measured and analyzed. Data are shown as median ± interquartile range. The Mann-Whitney U *t*test was performed.